

1
2
3
4
5
6
7
8
9
10
11
12
13
14
15
16
17
18
19
20

Complex collective dynamics of active torque-driven colloids at interfaces

Alexey Snezhko

*Materials Science Division, Argonne National Laboratory, 9700 S. Cass Avenue, Argonne,
IL 60564, USA*

Abstract

21
22
23
24
25
26
27
28
29
30
31
32
33
34
35
36
37
38
39
40
41
42
43
44
45
46

Modern self-assembly techniques aiming to produce complex structural order or functional diversity often rely on non-equilibrium conditions in the system. Light, electric or magnetic fields are predominantly used to modify interaction profiles of colloidal particles during self-assembly or induce complex out-of-equilibrium dynamic ordering. The energy injection rate, and properties of the environment are important control parameters that influence the outcome of active (dynamic) self-assembly. The current review is focused on a case of collective dynamics and self-assembly of particles with externally driven torques coupled to a liquid or solid interface. The complexity of interactions in such systems is further enriched by strong hydrodynamic coupling between particles. Unconventionally ordered dynamic self-assembled patterns, spontaneous symmetry breaking phenomena, self-propulsion and collective transport have been reported in torque-driven colloids. Some of the features of the complex collective behavior and dynamic pattern formation in those active systems have been successfully captured in simulations.

Keywords: collective dynamics, dynamic self-assembly, rotors

50
51
52
53
54
55
56
57
58

¹e-mail address: snezhko@anl.gov

1
2
3
4
5
6
7
8
9 **1. Introduction**

10
11 Self-assembled colloidal structures and materials capable of supporting struc-
12 tural complexity and functional diversity must consume energy from the envi-
13 ronment and as a result remain out-of-equilibrium [1, 2]. Such dissipative
14 self-assembly is often called dynamic or active self-assembly [1] in contrast to
15 more conventional static assembly happening at or near thermodynamic equi-
16 librium [3, 4, 5, 6, 7].

17
18
19
20
21 A significant work has been dedicated to various aspects of equilibrium col-
22 loidal structures obtained as a result of static self-assembly [8, 9, 10, 11, 12, 13,
23 14, 15, 16, 17, 18, 19, 20, 21, 22, 23]. Static magnetic and electric fields have been
24 successfully used to direct and control the self-assembly processes through in-situ
25 modification of particle interactions [24, 25, 26, 27, 28, 29, 30, 31, 32, 33, 34, 35].
26 It allowed to slightly expend the amount of available self-assembled structures.
27 Once formed these assemblies do not require an external energy to sustain the
28 structure. In contrast, dynamically assembled structures rely on external en-
29 ergy input and cease to exist once the energy source is removed. Due to the
30 fact that these externally driven particles are not in thermodynamic equilib-
31 rium, these dynamically assembling systems are called 'active'. Alternating
32 electric/magnetic fields demonstrated the potential to introduce dynamics into
33 the self-assembly process and number of nontrivially ordered dynamic structures
34 have been reported [36, 37, 38, 39, 40, 41, 42, 43, 44, 45, 46, 47, 48, 49, 50].
35 Remarkable toroidal vortices and pulsating rings have been reported in elec-
36 tric field driven colloidal ensemble comprised of conductive spherical particles
37 in low-electrolyte liquids [50]. Dynamic two-dimensional hexagonal sheets as-
38 sembled in rotating magnetic [38, 51] or electric [47] fields were observed in
39 suspensions of paramagnetic and PMMA particles, respectively. Particle foams,
40 honeycomb-structured composites and complex dynamic vortex patterns have
41 been reported in triaxial time-varying magnetic fields [38, 52]. Dynamically
42 assembled colloidal structures "living" outside of equilibrium have made ac-
43 cessible properties that are usually attributed to biological systems, such as
44
45
46
47
48
49
50
51
52
53
54
55
56
57
58
59
60
61
62
63
64
65

1
2
3
4
5
6
7
8
9 self-healing [42]. In all scenarios of the dynamic self-assembly in colloidal sus-
10 pensions the observed dynamic patterns are often a result of a fine-tuned dy-
11 namic balance between magnetic/electric dipole interactions, steric repulsions
12 and induced hydrodynamic flows.
13
14

15 The present paper reviews a less conventional case of collective dynamics
16 and self-assembly of particles with externally driven torques coupled to a liquid
17 or solid interface. Hydrodynamic interactions are believed to play a crucial
18 role in the onset of collective dynamics and pattern formation in torque driven
19 suspensions.
20
21
22
23

24 **2. Magnetic field assisted torque driven particles: collective dynamics** 25 **and self-assembly** 26 27

28 Magnetic field is an effective tool to exert torques on any material with mag-
29 netic moment (permanent or induced). One of the first realizations of torque-
30 driven dynamic self-assembly powered by a magnetic field was accomplished
31 in a system of magnetized millimeter-sized discs suspended at a liquid-air in-
32 terface and subjected to a rotating field produced by a rotating permanent
33 magnet [53, 54]. The disks were spinning around their axis with the frequency
34 of the permanent magnet, see Figure 1. The fluid motion associated with the
35 disk spinning induced repulsive hydrodynamic interactions between spinning
36 disks. The competition between axisymmetric magnetic attraction and hydro-
37 dynamic repulsion of the disks let to the formation of a number of dynamic pat-
38 terns exhibiting various types of ordering [53, 54]. Experiments clearly demon-
39 strated that inertial effects are significant in such system (the Reynolds number,
40 $Re = \rho\omega a^2/\mu < O(1)$, is small but finite). Each particle experience a lift force
41 transverse to the streamlines. Hydrodynamic repulsion facilitated by the lift
42 forces balances the time averaged magnetic attraction and leads to a formation
43 of steady dynamic patterns. Each particle dissipates energy supplied by the
44 external rotating magnetic field while maintaining dynamic order. Frequency
45 of the rotating magnetic field can be tuned to adjust the force balance in the
46
47
48
49
50
51
52
53
54
55
56
57
58
59
60
61
62
63
64
65

1
2
3
4
5
6
7
8
9 system and resulting dynamically assembled patterns [53, 54].

10 Magnetic particles with pinned (or fixed) magnetic moments automatically
11 have a potential to be torque-actuated in alternating magnetic fields in con-
12 trast to paramagnetic particles that acquire magnetic moment along the field
13 direction only when subject to the external magnetic field. Ferromagnetic sus-
14 pensions proved to be a scientifically rich systems to study collective dynamics
15 and self-assembly in active torque-driven ensembles [43, 2].

16
17 Ferromagnetically ordered particles subjected to a uniform constant mag-
18 netic field experience a torque, forcing their magnetic moment to be aligned
19 with the applied field direction. There are two scenarios on how a ferromag-
20 netic particle can change magnetic moment orientation: (a) it can rotate mag-
21 netic moment inside the particle by an adjustment of the internal magnetic
22 domain structure, or (b)mechanically adjust orientation of the particle to align
23 the magnetic moment with the external field direction. In a typical ferromag-
24 netic microparticle magnetic domain walls are pinned by the internal defects and
25 reorientation of its movement is often associated with high energy losses. As a
26 consequence, in most cases it is more energetically favorable for a ferromagnetic
27 microparticle at a liquid interface (where the friction is low) to proceed with the
28 mechanism (b) and mechanically adjust the orientation of the particle('magnetic
29 shaking') [45]. During this process we transfer the particle's torque to the lo-
30 cal excitations of the liquid interface and induce vortical hydrodynamic flows
31 around each particle.

32
33 Maintained in a state away-from-equilibrium by application of an alternat-
34 ing (*ac*) magnetic fields, a magnetic colloidal suspension at liquid interfaces
35 exhibits a strong tendency towards dynamic self-organization [43, 37]. Two dis-
36 tinctive geometries of the torque-driven actuation of particles are possible for
37 ferromagnetic suspension at liquid interfaces: a) alternating magnetic field is
38 perpendicular to the interface [55], and b) alternating field is along the inter-
39 face [56].
40
41
42
43
44
45
46
47
48
49
50
51
52
53
54
55
56
57
58
59
60
61
62
63
64
65

1
2
3
4
5
6
7
8
9 *2.1. Dynamic assembly of particles driven by a magnetic field transversal to the*
10 *liquid interface*

11
12 In a transverse orientation (the alternating field axis is perpendicular to
13 the liquid interface) astounding dynamically assembled structures (see Fig. 2)
14 emerge in a certain range of excitation parameters (magnetic field amplitude
15 and frequency) [45].
16

17
18 These structures are dynamic by nature and exist only while we supply
19 energy by means of an external driving field. Once formed the patterns are sta-
20 ble provided the driving field is unchanged. Each structure is composed out of
21 segments; each segment consists of ferromagnetically aligned chains of micropar-
22 ticles whose magnetic moments are aligned along the chain direction. The seg-
23 ments, however, are anti-ferromagnetically aligned: the total magnetic moment
24 per segment reverses its direction from section to section as demonstrated in the
25 Figure 2(c). Amazingly, the long-range order has a completely unconventional
26 origin. It is facilitated by a structure-induced surface wave [55, 45, 57].
27
28

29
30 In the process of dynamic self-assembly, ferromagnetic suspensions at liquid-
31 air interfaces often develop strong large-scale hydrodynamic surface flows in the
32 vicinity of assembled structures [58]. The strongest flows are concentrated at
33 opposite ends of the dynamic pattern where the centers of the vortices are
34 located (dark spots in Figure 3(a)). The flow velocity can be as fast as a
35 few centimeters per second and is controlled by the frequency of the driving
36 magnetic field. It was demonstrated that under certain conditions [39] the re-
37 ported dynamic structures spontaneously break the symmetry of self-generated
38 surface flows and turn into self-propelled entities, Figure 3(b). This type of
39 magnetic surface swimmer is rather unique due to the unusual mechanism of
40 self-propulsion exploiting symmetry breaking of self-generated surface flows and
41 the intrinsic antiferromagnetic nature of the swimmer's structure, in contrast
42 to previously reported colloidal swimmers [59, 60]. In multiple-swimmers state,
43 dynamic self-assembled swimmers create a highly disordered and non-periodic
44 surface velocity field [61] with Kolmogorov energy spectra that are character-
45 istic of two dimensional systems; this result indicates that self-generated flows
46
47
48
49
50
51
52
53
54
55
56
57
58
59
60
61
62
63
64
65

1
2
3
4
5
6
7
8
9 are highly localized near the interface.

10 One of the key ingredients facilitating active self-assembly of ferromagnetic
11 suspensions at liquid-air interfaces and leading to the formation of magnetic
12 snakes has been hydrodynamic long-range interactions produced by particles.
13 Consequently, modification of this component of particle interactions provides
14 an efficient tool to modify and control the results of dynamic assembly. Changes
15 in the interface liquid-air viscosity [62] or introduction of a top liquid layer
16 (liquid-liquid interface) [37] produces another remarkable self-assembled dy-
17 namic structures - localised asters- illustrated in Fig. 4.

18 Dynamic self-assembly in this system is caused by the interactions between
19 ferromagnetic particles responding to an external periodic magnetic field (mag-
20 netic torque transfer) and both self-induced interface deformations and hydro-
21 dynamic flows in the bulk of the liquids [37]. A short-range magnetic order,
22 governed by dipole-dipole magnetic interactions between the particles, promotes
23 formation of chains. Self-induced hydrodynamic flows with non-negligible fluid
24 inertia (typical Reynolds number for asters is of the order of 10) and waves pro-
25 vide a necessary feedback mechanism that leads to the formation of asters.

26 The arrangement of chains within an aster is governed by the self-induced hy-
27 drodynamic flows and dipole-dipole repulsion of chains. In contrast to magnetic
28 snakes observed at liquid-air interfaces [45, 55, 39], a presence of a top liquid
29 drastically changes the overall force balance and, correspondingly, the outcome
30 of a dynamic self-assembly. An excited circular wave leads to a formation of
31 radial ordering of the magnetic chains, and the chains decorate slopes of the
32 self-induced circular standing wave. Asters are composed of ferromagnetically
33 ordered chains of microparticles decorating circular interfacial wave (the asters
34 net magnetic moment is zero). This arrangement implies two permissible mag-
35 netic configurations (flavors): magnetic moments pointing inward, towards the
36 center of the aster, and outward (anti-aster), Fig.4b. Both flavors are usually
37 present in the system.

38 Asters generate large-scale three-dimensional toroidal flows in both liquids
39 (or in the bottom layer in case of liquid-air interface of high viscosity [62]) as
40
41
42
43
44
45
46
47
48
49
50
51
52
53
54
55
56
57
58
59
60
61
62
63
64
65

1
2
3
4
5
6
7
8
9 shown in Fig. 5. This result is in a stark contrast to the quasi-two dimensional
10 flows created by magnetic snakes at a liquid-air interface [58]. Fluid jets, point-
11 ing perpendicular to the interface, emanate in both top and bottom liquids.
12 Figure 5a,b shows the amplitude of the flow velocities created by an aster in the
13 bottom liquid (flow in the upper layer has similar structure). The jet's velocity
14 can reach a magnitude up to 2 cm/s and depends on the frequency of the applied
15 magnetic field (higher frequency yields faster jet flows).
16
17
18
19

20 Dynamic order and hydrodynamic flows are tightly bound to each other due
21 to a fine balance between particle interactions and self-induced streaming flows.
22 The aster's shape change in response to external stimuli (static in-plane field)
23 results in a controlled collective locomotion of asters facilitated by hydrodynamic
24 jets rather than a magnetic force [37].
25
26
27
28

29 *2.2. Collective dynamics and assembly triggered by an in-plane field actuation*

30

31 Yet another fascinating realization of a torque-driven active self-assembly
32 comes from a seemingly trivial system (it was also initially overlooked and fil-
33 tered out by the author due to 'apparent' triviality)- suspension of ferromagnetic
34 particles at liquid interface energized by alternating field in-plane with the in-
35 terface (fig. 6a). Kept at out-of-equilibrium condition by alternating uniaxial
36 magnetic field the system demonstrates remarkable complexity [56].
37
38
39

40 Surface tension confines the ferromagnetic particles with intrinsically pinned
41 magnetic moments to the surface of the water-air interface. An alternating mag-
42 netic field applied parallel to the interface exerts torque on them. The torque is
43 dissipated locally in the liquid and generates hydrodynamic flows around each
44 particle. Consequently, the particles interact by two temporally related, but
45 physically distinct types of forces: magnetic (dipole-dipole interactions) and
46 hydrodynamic. Dynamic self-assembly reflects the interplay between magnetic
47 interactions and hydrodynamic flows. The relative contributions of these two
48 primary interactions are modulated by the parameters of the energizing alter-
49 nating magnetic field [56, 63]. As a result, the system exhibits a remarkable
50 diversity of quasi-stable active states that are dynamic, and exist only while
51
52
53
54
55
56
57
58

1
2
3
4
5
6
7
8
9 energy is supplied by the *ac* magnetic field.

10 Loose clusters (Fig. 6b) extended along the *ac* magnetic field are formed at
11 low frequencies . The clusters exhibit periodic changes in shape (pulsations):
12 over time the cluster extends and contracts with a fraction of the driving mag-
13 netic field frequency. At elevated frequencies of the applied field, the clusters
14 transform into a cloud of continuously rearranging short chains (Fig. 6c). In
15 striking contrast with loose clusters, the cloud switches the axis of elongation
16 and extends perpendicular to the *ac* magnetic field. Further increase in the
17 frequency yields a new remarkable dynamic phase: spinners (see Fig. 6d). The
18 spinners emerge via spontaneous breaking of the uniaxial symmetry of the ener-
19 gizing magnetic field. In this phase the particles self-assemble into short chains,
20 and rotate in the plain of the air-water interface at the frequency of the applied
21 *ac* magnetic field. This rotation creates strong in-plane hydrodynamic flows, see
22 Fig. 6f,g. The spinners exhibit complex dynamic behavior: they move across
23 the surface, collide, disintegrate, and re-assemble [56, 63]. The multi-spinner
24 state (gas) has no apparent preferred direction and covers the entire area of the
25 container uniformly. At higher frequencies of the applied field the spinners give
26 way to dynamic wires (see Fig. 6e). All phases form and disassemble reversibly.

27
28
29
30
31
32
33
34
35
36
37 Dynamic spinners are composed of short self-assembled chains of micro-
38 particles ferromagnetically ordered due to the prevailing magnetic dipole-dipole
39 inter-particle interactions. Spinners rotate clockwise or counterclockwise with
40 the frequency of the applied field. Since for the case of uniaxial magnetic field
41 the clock/counterclockwise senses of rotation are equally probable, the initial
42 direction is selected by a variety of factors, like interactions with neighboring
43 particles and flows. The rotating chains exert viscous torques on the liquid
44 which trigger strong long-range [64] hydrodynamic vortical flows at the interface.
45 Spinners move (seemingly randomly) due to magnetic interactions and the flows
46 generated by other spinners. Their collective motion creates an overall gas-like
47 appearance of the phase. These rotors collide, disintegrate and reassemble, and
48 thus create complex time-dependent hydrodynamic patterns at the interface.
49
50
51
52
53
54
55
56
57
58
59
60
61
62
63
64
65

1
2
3
4
5
6
7
8
9
10
11
12
13
14
15
16
17
18
19
20
21
22
23
24
25
26
27
28
29
30
31
32
33
34
35
36
37
38
39
40
41
42
43
44
45
46
47
48
49
50
51
52
53
54
55
56
57
58
59
60
61
62
63
64
65

2.3. Driven magnetic Janus colloids

Torque-assisted active self-assembly has been reported also in ensembles of magnetic Janus colloids [41, 65]. By applying a precessing field to spherical silica particles with a thin nickel film directionally deposited onto one of their hemispheres the magnetic torques were generated that drove the particles to spin around the precession axis and oscillate perpendicular to the rotating plane, Fig. 7a. Subjected to precessing fields magnetic Janus particles demonstrated tendency towards synchronization [41]. At low precession angles long virtually defect-free microtubes spontaneously formed in suspension of these Janus spheres, see Fig. 7b. Structurally these microtubes were achiral and consisted of a staggered set of regular polygons. Once formed these microtubes rolled on the substrate with spheres remained in continual motion. Additional dynamics induced transitions with the frequency of the precessing field have been observed [41].

One of the useful features of the magnetic Janus particles is a shifted dipole moment with respect to a geometrical center of the particle. Recent computer simulation results of the cluster structures in systems of particles with shifted magnetic dipole moments suggested an importance of this additionally introduced anisotropy for the topology of assembled clusters [66, 67]. Subjected to time-varying fields this tunable property could be used to control complex dynamics of the suspension and an outcome of the dynamic assembly. The shift of the magnetic dipole from the geometrical center of a particle depends on the directional coating thickness. The thinner the film the larger the dipole offset from the center [65]. In rotating magnetic fields of moderate strength (2-5mT) magnetic Janus spheres assembled in extended hexagonal planar crystals (Fig. 8) that rotate as a whole with an angular velocity that is fraction of the rotational field [65]. At elevated strengths of the rotational field (about 30mT) unexpected dynamic transition has been observed: single particles formed dumbbells with their magnetic hemispheres pointing inward, see Fig. 8c. Once formed, dicolloids start to rotate around their center of mass. In rotating magnetic fields these dicolloids retain hexagonal symmetry with lattice constant twice as large as that

1
2
3
4
5
6
7
8
9 for single particles [65], Fig. 8. Denser aggregates of the dicolloids exhibit more
10 complex dynamic packing, see Fig. 8d.

11
12 Janus spherical particles have demonstrated a rich variety of dynamic col-
13 loidal superstructures when driven by magnetic torques. Control of the magnetic
14 coating thickness allowed precise tuning of magnetic properties of Janus colloids
15 which govern the symmetry of the resulting dynamic assemblies.
16
17
18
19

20 **3. Quincke rollers: electric field assisted torque driven colloids**

21
22 Electric field can also be used to exert mechanical torque on colloids tak-
23 ing advantage of electrohydrodynamic phenomenon known as Quincke rota-
24 tion [68, 69]. Above a certain critical electric field applied to an insulating
25 sphere immersed in a conducting liquid spontaneous symmetry breaking of the
26 charge distribution at the sphere’s surface results in a net electrostatic torque
27 that causes the sphere to rotate in a random direction perpendicular to the
28 applied field and also generating hydrodynamic torques in the media. This
29 instability can be effectively exploited to generate large ensembles of rotating
30 particles to tune rheological properties of suspensions [70, 71] and create large
31 ensembles of active self-propelled colloids at solid interfaces [72, 73].
32
33
34
35
36
37

38 At low densities the rollers formed an isotropic gas-like phase. As area frac-
39 tion of rollers increases above some critical density a macroscopic fraction of
40 rollers self-organizes in a band and cruise in the same direction, see Fig. 9b. No
41 stationary state involving more than one band has been observed. Remarkably,
42 the velocity of the band (or colloidal flock) is found to be close to the single
43 particle velocity at the front of the band. Comparison of experiments with theo-
44 retical prediction suggests that hydrodynamic interactions promote and protect
45 the formation of macroscopic bands at low densities and homogeneous polar
46 phases at high densities [72].
47
48
49
50
51

52 Being subjected to an additional boundary constraints (convex polygonal
53 regions) Quincke rollers may develop a non-equilibrium phase transition into
54 heterogeneous vortex state [73], see Fig. 10. As the area fraction of rollers in
55
56
57
58

1
2
3
4
5
6
7
8
9 the confinement increases above some threshold value, collective motion emerges
10 spontaneously in the system. Globally ordered state with equally probable left-
11 and right-handed vortices sets in the colloidal ensemble. It was also shown that
12 this vortex state of the system is not very sensitive to a specific geometry of the
13 boundary and rather is a genuine state of the polar active matter [73].
14
15
16
17

18 **4. Theoretical aspects**

19
20
21 Dynamics of driven suspensions of ferromagnetically ordered particles has
22 been investigated by means of Brownian dynamics (BD) computer simulations [74,
23 75]. There for the case of a bulk system without a hydrodynamic coupling a
24 full non-equilibrium phase diagram as a function of the driving frequency and
25 field strength has been constructed. Appearance of the layered states (similar
26 to previously reported in the system of induced dipoles [76]) has been cap-
27 tured in simulations. Implementation of the hydrodynamic interactions in a
28 quasi-two-dimensional setup in a presence of a rotational driving magnetic field
29 allowed to access and study in detail the interplay between permanent dipolar
30 and hydrodynamic interactions [75]. Results indicated a profound effect of the
31 hydrodynamic interactions on the dynamics of structure formation and behavior
32 of the assembled clusters.
33
34
35
36
37
38
39

40 A number of studies have become available that theoretically investigate col-
41 lective effects in suspensions of particles driven by a Quincke rotation [77, 78].
42 Within a mean field approximation considering the dynamics of particle orien-
43 tations in the flow induced by rotating particles a non-equilibrium transition to
44 the polar order at sufficiently high concentration of particles has been estab-
45 lished [78].
46
47
48

49 Some of the aspects of the torque driven dynamics of particles at liquid
50 interfaces has been captured by simulations within Stokes approximation (neg-
51 ligible inertia) [79, 80]. In contrast, the investigation of active rotors in the ab-
52 sence of the hydrodynamic interactions resulted in phase separation of spinners
53 (clockwise-counterclockwise direction) via spinodal decomposition as well as for-
54
55
56
57
58
59
60
61
62
63
64
65

1
2
3
4
5
6
7
8
9 mation of rotating clusters [81]. Most experiments with active rotors strongly
10 suggest the importance of the fluid inertia in the formation of the dynamic or-
11 der [43, 53]. While the Reynolds number is usually considered low and often
12 of the order of unity in those experiments, the effects of the flows associated
13 with the fluid inertia (such as the Magnus force) are crucial for the resulting
14 collective dynamics and order formation in the active torque-driven ensembles.
15 Thus, in order to capture the relevant physical behavior of the systems with
16 active rotors Navier-Stokes equation has to be solved with finite Reynolds num-
17 bers. A few computational algorithms have been successfully applied to tackle
18 the complex out-of-equilibrium dynamic of active rotors in 2d. Fluid particle
19 dynamics (FPD) method [82], force coupling method (FCM) [83, 84], multipar-
20 ticle collision dynamics (MPC) scheme [85] and Fourier spectral method [86]
21 have been used to treat hydrodynamics in such systems. Hybrid simulations
22 combining fluid dynamics with Molecular Dynamics (MD) for particles [87, 86],
23 fluid particle dynamics method [88] and force coupling method [89] were able to
24 capture in detail the essential dynamics and order formation of the active rotors
25 at 2d interfaces, see Fig. 11.
26
27
28
29
30
31
32
33
34
35
36

37 **5. Summary and outlook**

38
39 Torque driven particles demonstrate remarkably diverse dynamics and tun-
40 able active self-assembly. Up to recent years they have been rarely the sub-
41 ject of the detailed studies in a context of out-of-equilibrium self-assembly and
42 self-propulsion. Ensembles of torque driven particles exhibit complex collective
43 behavior often reminiscent of a more 'conventional' active particle systems such
44 as synthetic self-propelled particles [90, 91, 92, 93] or bacteria [94, 95]. Un-
45 derstanding the fundamental principles guiding out-of-equilibrium dynamics in
46 torque-driven system will add an essential tool in a toolbox for assembly of novel
47 materials which might exhibit the multi-level functionality and hierarchical or-
48 ganization that up to now are only found in biological world. Smart materials
49 that can adjust their shape and functionality in response to external stimuli
50
51
52
53
54
55
56
57
58
59
60
61
62
63
64
65

1
2
3
4
5
6
7
8
9 offer an enormous potential for applications.

10 Significant progress in the last years has been made in the understanding of
11 a role the hydrodynamics plays in out-of-equilibrium systems. Effects of a fluid
12 inertia (small but finite Reynolds numbers) proved to be important and in most
13 of the cases crucial for understanding complex collective dynamics of particle
14 ensembles at the microscale. To date mostly spherical and disk-like particles
15 have been employed in the studies of active torque-driven systems. The use of
16 shape-anisotropic particles may significantly change the dynamic behavior and
17 outcome of the active self-assembly in the system since hydrodynamic feedback
18 of the particles strongly depends on the shape. This will likely be one of a
19 major research thrusts in the future. Also realization of a dynamic self-assembly
20 powered by torque transfer in three dimensions is a promising research area.

21
22
23
24
25
26
27
28 A few efficient computational schemes have been developed to capture hy-
29 drodynamic interactions in 2d geometries. A variety of dynamic phases was
30 reproduced and predicted in simulations. A great challenge is to develop more
31 refined models and algorithms incorporating realistic 3d hydrodynamics that to
32 date is still considered to be computationally prohibitive. Access to realistic
33 predictive modeling will enable to speed up and direct the search for future
34 smart materials with bio-mimetic functionalities.

35 36 37 38 39 40 **6. Acknowledgment**

41
42 This work was supported by the U.S. Department of Energy, Office of Sci-
43 ence, Basic Energy Sciences, Materials Sciences and Engineering Division.

44 45 46 47 **References**

- 48
49 [1] *G. Whitesides, B. Grzybowski, Self-assembly at all scales, *Science*
50 295 (5564) (2002) 2418–2421.
51
52
53 [2] *J. E. Martin, A. Snezhko, Driving self-assembly and emergent dynam-
54 ics in colloidal suspensions by time-dependent magnetic fields, *Reports on*
55 *Progress in Physics* 76 (12) (2013) 126601.
56
57
58

- 1
2
3
4
5
6
7
8
9 [3] J. J. Urban, D. V. Talapin, E. V. Shevchenko, C. R. Kagan, C. B. Murray,
10 Synergism in binary nanocrystal superlattices leads to enhanced p-type
11 conductivity in self-assembled pbte/ag2te thin films, *Nature Materials* 6 (2)
12 (2007) 115–121.
13
14
15 [4] O. D. Velev, E. W. Kaler, Structured porous materials via colloidal crystal
16 templating: from inorganic oxides to metals, *Advanced Materials* 12 (7)
17 (2000) 531–534.
18
19 [5] C. A. Mirkin, R. L. Letsinger, R. C. Mucic, J. J. Storhoff, et al., A dna-
20 based method for rationally assembling nanoparticles into macroscopic ma-
21 terials, *Nature* 382 (6592) (1996) 607–609.
22
23 [6] G. Subramanian, V. N. Manoharan, J. D. Thorne, D. J. Pine, Ordered
24 macroporous materials by colloidal assembly: a possible route to photonic
25 bandgap materials, *Advanced Materials* 11 (15) (1999) 1261–1265.
26
27 [7] A. van Blaaderen, Colloids under external control, *Mrs Bulletin* 29 (02)
28 (2004) 85–90.
29
30 [8] I. Muševič, M. Škarabot, U. Tkalec, M. Ravnik, S. Žumer, Two-dimensional
31 nematic colloidal crystals self-assembled by topological defects, *Science*
32 313 (5789) (2006) 954–958.
33
34 [9] D. Frenkel, D. J. Wales, Colloidal self-assembly: designed to yield, *Nature*
35 *materials* 10 (6) (2011) 410–411.
36
37 [10] A. Rugge, S. H. Tolbert, Effect of electrostatic interactions on crystalliza-
38 tion in binary colloidal films, *Langmuir* 18 (18) (2002) 7057–7065.
39
40 [11] F. Li, D. P. Josephson, A. Stein, Colloidal assembly: the road from parti-
41 cles to colloidal molecules and crystals, *Angewandte Chemie International*
42 *Edition* 50 (2) (2011) 360–388.
43
44 [12] S. C. Glotzer, M. J. Solomon, Anisotropy of building blocks and their
45 assembly into complex structures, *Nature materials* 6 (8) (2007) 557–562.
46
47
48
49
50
51
52
53
54
55
56
57
58

- 1
2
3
4
5
6
7
8
9 [13] S. C. Warren, L. C. Messina, L. S. Slaughter, M. Kamperman, Q. Zhou,
10 S. M. Gruner, F. J. DiSalvo, U. Wiesner, Ordered mesoporous materials
11 from metal nanoparticle–block copolymer self-assembly, *Science* 320 (5884)
12 (2008) 1748–1752.
13
14
15 [14] O. D. Velev, S. Gupta, Materials fabricated by micro-and nanoparticle
16 assembly—the challenging path from science to engineering, *Adv. Mater*
17 21 (19) (2009) 1897–1905.
18
19 [15] S. Sacanna, W. Irvine, P. M. Chaikin, D. J. Pine, Lock and key colloids,
20 *Nature* 464 (7288) (2010) 575–578.
21
22 [16] Q. Chen, S. C. Bae, S. Granick, Directed self-assembly of a colloidal kagome
23 lattice, *Nature* 469 (7330) (2011) 381–384.
24
25 [17] A. Yethiraj, J. H. Thijssen, A. Wouterse, A. van Blaaderen, Large-area
26 electric-field-induced colloidal single crystals for photonic applications, *Ad-*
27 *vanced materials* 16 (7) (2004) 596–600.
28
29 [18] R. M. Erb, H. S. Son, B. Samanta, V. M. Rotello, B. B. Yellen, Mag-
30 netic assembly of colloidal superstructures with multipole symmetry, *Nat-*
31 *ure* 457 (7232) (2009) 999–1002.
32
33 [19] D. Nykypanchuk, M. M. Maye, D. van der Lelie, O. Gang, Dna-guided
34 crystallization of colloidal nanoparticles, *Nature* 451 (7178) (2008) 549–
35 552.
36
37 [20] M. E. Leunissen, C. G. Christova, A.-P. Hynninen, C. P. Royall, A. I.
38 Campbell, A. Imhof, M. Dijkstra, R. Van Roij, A. Van Blaaderen, Ionic
39 colloidal crystals of oppositely charged particles, *Nature* 437 (7056) (2005)
40 235–240.
41
42 [21] J. C. Love, A. R. Urbach, M. G. Prentiss, G. M. Whitesides, Three-
43 dimensional self-assembly of metallic rods with submicron diameters using
44 magnetic interactions, *Journal of the American Chemical Society* 125 (42)
45 (2003) 12696–12697.
46
47
48
49
50
51
52
53
54
55
56
57
58

- 1
2
3
4
5
6
7
8
9 [22] X. Lin, R. Parthasarathy, H. Jaeger, Direct patterning of self-assembled
10 nanocrystal monolayers by electron beams, *Applied Physics Letters* 78 (13)
11 (2001) 1915–1917.
12
13 [23] Z. Zhang, S. C. Glotzer, Self-assembly of patchy particles, *Nano Letters*
14 4 (8) (2004) 1407–1413.
15
16 [24] C. P. Royall, E. C. Vermolen, A. van Blaaderen, H. Tanaka, Controlling
17 competition between crystallization and glass formation in binary colloids
18 with an external field, *Journal of Physics: Condensed Matter* 20 (40) (2008)
19 404225.
20
21 [25] H. Löwen, Colloidal dispersions in external fields: recent developments,
22 *Journal of Physics: Condensed Matter* 20 (40) (2008) 404201.
23
24 [26] J. Richardi, J. J. Weis, Low density mesostructures of confined dipolar
25 particles in an external field, *J. Chem. Phys.* 135 (2011) 124502.
26
27 [27] A. Snezhko, I. Aranson, W.-K. Kwok, Structure formation in electromag-
28 netically driven granular media, *Physical review letters* 94 (10) (2005)
29 108002.
30
31 [28] K. Zahn, G. Maret, Two-dimensional colloidal structures responsive to ex-
32 ternal fields, *Current opinion in colloid & interface science* 4 (1) (1999)
33 60–65.
34
35 [29] A. van Blaaderen, M. Dijkstra, R. van Roij, A. Imhof, M. Kamp, B. Kwaad-
36 gras, T. Vissers, B. Liu, Manipulating the self assembly of colloids in elec-
37 tric fields, *The European Physical Journal Special Topics* 222 (11) (2013)
38 2895–2909.
39
40 [30] S. Fraden, A. J. Hurd, R. B. Meyer, Electric-field-induced association of
41 colloidal particles, *Phys. Rev. Lett.* 63 (1989) 2373–2378.
42
43 [31] W. D. Ristenpart, I. A. Aksay, D. A. Saville, Electrically guided assembly
44 of planar superlattices in binary colloidal suspensions, *Phys. Rev. Lett.* 90
45 (2003) 128303.
46
47
48
49
50
51
52
53
54
55
56
57
58

- 1
2
3
4
5
6
7
8
9 [32] K.-Q. Zhang, X. Y. Liu, Controlled formation of colloidal structures by an
10 alternating electric field and its mechanisms, *J. Chem. Phys.* 130 (2009)
11 184901.
12
13
14 [33] M. Trau, D. A. Saville, I. A. Aksay, Field-induced layering of colloidal
15 crystals, *Science* 272 (5262) (1996) 706–709.
16
17
18 [34] A. P. Bartlett, A. K. Agarwal, A. Yethiraj, Dynamic templating of col-
19 loidal patterns in three dimensions with nonuniform electric fields, *Lang-*
20 *muir* 27 (8) (2011) 4313–4318.
21
22
23 [35] J. S. Park, D. Saintillan, Electric-field-induced ordering and pattern for-
24 mation in colloidal suspensions, *Phys. Rev. E* 83 (2011) 041409.
25
26
27 [36] * J. Martin, R. Anderson, C. Tigges, Thermal coarsening of uniaxial and
28 biaxial field-structured composites, *J. Chem. Phys.* 110 (10).
29
30
31 [37] * A. Snezhko, I. S. Aranson, Magnetic manipulation of self-assembled col-
32 loidal asters, *Nat. Mater.* 10 (9) (2011) 698–703.
33
34
35 [38] J. E. Martin, E. Venturini, G. L. Gulley, J. Williamson, Using triaxial
36 magnetic fields to create high susceptibility particle composites, *Phys. Rev.*
37 *E* 69 (2004) 021508.
38
39
40 [39] * A. Snezhko, M. Belkin, I. S. Aranson, W.-K. Kwok, Self-assembled mag-
41 netic surface swimmers, *Phys. Rev. Lett.* 102 (2009) 118103.
42
43
44 [40] P. Tierno, T. M. Fischer, T. H. Johansen, F. Sagués, Colloidal assembly on
45 magnetically vibrated stripes, *Phys. Rev. Lett.* 100 (2008) 148304.
46
47
48 [41] * J. Yang, M. Bloom, S. C. Bae, E. Luijten, S. Granick, Linking synchro-
49 nization to self-assembly using magnetic janus colloids, *Nature* 91 (2012)
50 578.
51
52
53 [42] * N. Osterman, I. Poberaj, J. Dobnikar, D. Frenkel, P. Zihlerl, D. Babić,
54 Field-induced self-assembly of suspended colloidal membranes, *Phys. Rev.*
55 *Lett.* 103 (2009) 228301.
56
57
58

- 1
2
3
4
5
6
7
8
9 [43] * A. Snezhko, Non-equilibrium magnetic colloidal dispersions at liquid-air
10 interfaces: dynamic patterns, magnetic order and self-assembled swimmers,
11 J. Phys.-Condens. Mat. 23 (15) (2011) 153101.
12
13
14 [44] A. Ray, S. Aliaskarisohi, T. M. Fischer, Dynamics of self-assembly of flower-
15 shaped magnetic colloidal clusters, Phys. Rev. E 82 (2010) 031406.
16
17
18 [45] * A. Snezhko, I. S. Aranson, W.-K. Kwok, Surface wave assisted self-
19 assembly of multidomain magnetic structures, Phys. Rev. Lett. 96 (2006)
20 078701.
21
22
23 [46] K. J. Solis, J. E. Martin, Isothermal magnetic advection: Creating func-
24 tional fluid flows for heat and mass transfer, Appl. Phys. Lett. 97 (2010)
25 034101.
26
27
28 [47] M. E. Leunissen, H. R. Vutukuri, A. van Blaaderen, Directing colloidal self-
29 assembly with biaxial electric fields, Adv. Mater. 21 (30) (2009) 0935–9648.
30
31
32
33 [48] A. Demortière, A. Snezhko, M. V. Sapozhnikov, N. Becker, T. Proslier,
34 I. S. Aranson, Self-assembled tunable networks of sticky colloidal particles,
35 Nature Communications 5 (2014) 3117.
36
37
38 [49] K. J. Solis, J. E. Martin, Complex magnetic fields breathe life into fluids,
39 Soft Matter 10 (45) (2014) 9136–9142.
40
41
42 [50] M. Sapozhnikov, Y. Tolmachev, I. Aranson, W. Kwok, Dynamic self-
43 assembly and patterns in electrostatically driven granular media, Phys.
44 Rev. Lett. 90 (2003) 114301.
45
46
47 [51] J. Martin, R. Anderson, R. Williamson, Generating strange magnetic and
48 dielectric interactions: Classical molecules and particle foams, J. Chem.
49 Phys. 118 (3) (2003) 1557–1570.
50
51
52 [52] J. E. Martin, K. J. Solis, Symmetry-breaking magnetic fields create a vortex
53 fluid that exhibits a negative viscosity, active wetting, and strong mixing,
54 Soft Matter 10 (22) (2014) 3993–4002.
55
56
57
58

- 1
2
3
4
5
6
7
8
9 [53] * B. Grzybowski, H. Stone, G. Whitesides, Dynamic self-assembly of mag-
10 netized, millimetre-sized objects rotating at a liquid–air interface, *Nature*
11 405 (6790) (2000) 1033–1036.
12
13
14 [54] B. A. Grzybowski, H. A. Stone, G. M. Whitesides, Dynamics of self assem-
15 bly of magnetized disks rotating at the liquid–air interface, *Proceedings of*
16 *the National Academy of Sciences* 99 (7) (2002) 4147–4151.
17
18 [55] A. Snezhko, I. S. Aranson, W.-K. Kwok, Dynamic self-assembly of magnetic
19 particles on the fluid interface: Surface-wave-mediated effective magnetic
20 exchange, *Phys. Rev. E* 73 (2006) 041306.
21
22 [56] * G. Kokot, D. Piet, G. M. Whitesides, I. S. Aranson, A. Snezhko, Emer-
23 gence of reconfigurable wires and spinners via dynamic self-assembly, *Sci-*
24 *entific Reports* 5 (2015) 9528. doi:10.1038/srep09528.
25
26 [57] A. Snezhko, I. S. Aranson, Magnetic properties of novel dynamic self-
27 assembled structures generated on the liquid/air interface, *Phys. Lett. A*
28 363 (5-6) (2007) 337–340.
29
30 [58] M. Belkin, A. Snezhko, I. S. Aranson, W.-K. Kwok, Driven magnetic par-
31 ticles on a fluid surface: Pattern assisted surface flows, *Phys. Rev. Lett.* 99
32 (2007) 158301.
33
34 [59] R. Dreyfus, J. Baudry, M. Roper, M. Fermigier, H. Stone, J. Bibette, Mi-
35 croscopic artificial swimmers, *Nature* 437 (7060) (2005) 862–865.
36
37 [60] S. Gangwal, O. J. Cayre, M. Z. Bazant, O. D. Velev, Induced-charge
38 electrophoresis of metallodielectric particles, *Phys. Rev. Lett.* 100 (2008)
39 058302.
40
41 [61] M. Belkin, A. Snezhko, I. S. Aranson, W.-K. Kwok, Magnetically driven
42 surface mixing, *Phys. Rev. E* 80 (2009) 011310.
43
44 [62] D. Piet, A. Straube, A. Snezhko, I. Aranson, Viscosity control of the dy-
45 namic self-assembly in ferromagnetic suspensions, *Physical Review Letters*
46 110 (19) (2013) 198001.
47
48
49
50
51
52
53
54
55
56
57
58

- 1
2
3
4
5
6
7
8
9 [63] * G. Kokot, A. Snezhko, I. S. Aranson, Emergent coherent states and flow
10 rectification in active magnetic colloidal monolayers, *Soft Matter* 9 (29)
11 (2013) 6757–6760.
12
13
14 [64] A. Snezhko, I. S. Aranson, Velocity statistics of dynamic spinners in out-of-
15 equilibrium magnetic suspensions, *Soft Matter* 11 (30) (2015) 6055–6061.
16
17 [65] * J. Yan, S. C. Bae, S. Granick, Colloidal superstructures programmed into
18 magnetic janus particles, *Advanced Materials* 27 (5) (2015) 874–879.
19
20 [66] M. Klinkigt, R. Weeber, S. Kantorovich, C. Holm, Cluster formation in
21 systems of shifted-dipole particles, *Soft Matter* 9 (2013) 3535–3546.
22
23 [67] A. I. Abrikosov, S. Sacanna, A. P. Philipse, P. Linse, Self-assembly of spher-
24 ical colloidal particles with off-centered magnetic dipoles, *Soft Matter* 9
25 (2013) 8904–8913.
26
27 [68] G. Quincke, Ueber rotationen im constanten electrischen felde, *Ann. Phys.-*
28 *Berlin* 295 (1896) 417–486.
29
30 [69] J. Melcher, G. Taylor, Electrohydrodynamics: a review of the role of in-
31 terfacial shear stresses, *Annual Review of Fluid Mechanics* 1 (1) (1969)
32 111–146.
33
34 [70] L. Lobry, E. Lemaire, Viscosity decrease induced by a dc electric field in a
35 suspension, *Journal of electrostatics* 47 (1) (1999) 61–69.
36
37 [71] N. Pannacci, E. Lemaire, L. Lobry, Rheology and structure of a suspension
38 of particles subjected to quincke rotation, *Rheologica Acta* 46 (7) (2007)
39 899–904.
40
41 [72] * A. Bricard, J.-B. Caussin, N. Desreumaux, O. Dauchot, D. Bartolo, Emer-
42 gence of macroscopic directed motion in populations of motile colloids, *Nature*
43 503 (7474) (2013) 95–98.
44
45
46
47
48
49
50
51
52
53
54
55
56
57
58
59
60
61
62
63
64
65

- 1
2
3
4
5
6
7
8
9 [73] * A. Bricard, J.-B. Caussin, D. Das, C. Savoie, V. Chikkadi, K. Shitara,
10 O. Chepizhko, F. Peruani, D. Saintillan, D. Bartolo, Emergent vortices in
11 populations of colloidal rollers, *Nature Communications* 6 (2015) 7470.
12
13
14 [74] S. Jager, S. H. L. Klapp, Pattern formation of dipolar colloids in rotating
15 fields: layering and synchronization, *Soft Matter* 7 (2011) 6606–6616.
16
17 [75] S. Jger, H. Stark, S. H. L. Klapp, Dynamics of cluster formation in driven
18 magnetic colloids dispersed on a monolayer, *Journal of Physics: Condensed*
19 *Matter* 25 (19) (2013) 195104.
20
21 [76] J. Martin, R. Anderson, C. Tigges, Simulation of the athermal coarsening
22 of composites structured by a biaxial field, *J. Chem. Phys.* 108 (18) (1998)
23 7887–7900.
24
25 [77] Y. Dolinsky, T. Elperin, Dipole interaction of the quince rotating particles,
26 *Phys. Rev. E* 85 (2012) 026608.
27
28 [78] M. Belovs, A. Cēbers, Relaxation of polar order in suspensions with quince
29 effect, *Phys. Rev. E* 89 (2014) 052310.
30
31 [79] K. Yeo, E. Lushi, P. M. Vlahovska, Collective dynamics in a binary mixture
32 of hydrodynamically coupled microrotors, *Physical Review Letters* 114 (18)
33 (2015) 188301.
34
35 [80] I. Llopis, I. Pagonabarraga, Hydrodynamic regimes of active rotators at
36 fluid interfaces, *The European Physical Journal E* 26 (1-2) (2008) 103–113.
37
38 [81] N. H. P. Nguyen, D. Klotsa, M. Engel, S. C. Glotzer, Emergent collective
39 phenomena in a mixture of hard shapes through active rotation, *Phys. Rev.*
40 *Lett.* 112 (2014) 075701.
41
42 [82] H. Tanaka, T. Araki, Simulation method of colloidal suspensions with hy-
43 drodynamic interactions: Fluid particle dynamics, *Physical Review Letters*
44 85 (6) (2000) 1338.
45
46
47
48
49
50
51
52
53
54
55
56
57
58
59
60
61
62
63
64
65

- 1
2
3
4
5
6
7
8
9 [83] M. Maxey, B. Patel, Localized force representations for particles sediment-
10 ing in stokes flow, *International Journal of Multiphase Flow* 27 (9) (2001)
11 1603–1626.
12
13
14 [84] S. Lomholt, M. R. Maxey, Force-coupling method for particulate two-phase
15 flow: Stokes flow, *Journal of Computational Physics* 184 (2) (2003) 381–
16 405.
17
18
19 [85] A. Malevanets, R. Kapral, Mesoscopic model for solvent dynamics, *The*
20 *Journal of Chemical Physics* 110 (17) (1999) 8605–8613.
21
22
23 [86] * M. Belkin, A. Glatz, A. Snezhko, I. S. Aranson, Model for dynamic self-
24 assembled magnetic surface structures, *Phys. Rev. E* 82 (2010) 015301.
25
26
27 [87] * I. O. Götze, G. Gompper, Dynamic self-assembly and directed flow of
28 rotating colloids in microchannels, *Physical Review E* 84 (3) (2011) 031404.
29
30
31 [88] * Y. Goto, H. Tanaka, Purely hydrodynamic ordering of rotating disks at
32 a finite reynolds number, *Nature Communications* 6.
33
34
35 [89] * E. Climent, K. Yeo, M. R. Maxey, G. E. Karniadakis, Dynamic self-
36 assembly of spinning particles, *Journal of Fluids Engineering* 129 (4) (2007)
37 379–387.
38
39
40 [90] S. Gangwal, O. J. Cayre, M. Z. Bazant, O. D. Velev, Induced-charge
41 electrophoresis of metallodielectric particles, *Phys. Rev. Lett.* 100 (2008)
42 058302.
43
44
45 [91] I. Buttinoni, J. Bialké, F. Kümmel, H. Löwen, C. Bechinger, T. Speck,
46 Dynamical clustering and phase separation in suspensions of self-propelled
47 colloidal particles, *Phys. Rev. Lett.* 110 (2013) 238301.
48
49
50 [92] H.-R. Jiang, N. Yoshinaga, M. Sano, Active motion of a janus particle by
51 self-thermophoresis in a defocused laser beam, *Phys. Rev. Lett.* 105 (2010)
52 268302.
53
54
55
56
57
58
59
60
61
62
63
64
65

- 1
2
3
4
5
6
7
8
9 [93] I. Theurkauff, C. Cottin-Bizonne, J. Palacci, C. Ybert, L. Bocquet, Dy-
10 namic clustering in active colloidal suspensions with chemical signaling,
11 Phys. Rev. Lett. 108 (2012) 268303.
12
13
14 [94] A. Sokolov, I. S. Aranson, J. O. Kessler, R. E. Goldstein, Concentration de-
15 pendence of the collective dynamics of swimming bacteria, Physical Review
16 Letters 98 (15) (2007) 158102.
17
18
19 [95] H. P. Zhang, A. Beer, E.-L. Florin, H. L. Swinney, Collective motion
20 and density fluctuations in bacterial colonies, Proceedings of the National
21 Academy of Sciences 107 (31) (2010) 13626–13630.
22
23
24
25
26
27
28
29
30
31
32
33
34
35
36
37
38
39
40
41
42
43
44
45
46
47
48
49
50
51
52
53
54
55
56
57
58
59
60
61
62
63
64
65

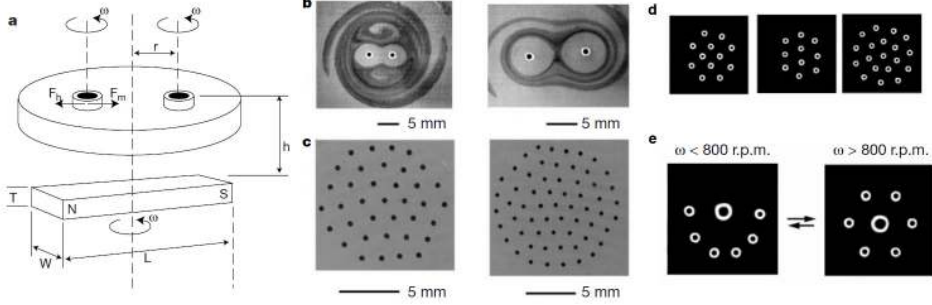


Figure 1: Dynamic assembly of rotating disks at a liquid-air interface. a) A scheme of the experiment. A rotating with angular velocity ω bar magnet is used to drive magnetic disks placed on the liquid-air interface. The streamlines are visualized by placing drops of rodamine/water solution. b) Two 1.27mm disks spinning at the ethylene glycol-water interface. Left panel: disks are at 700 rpm; Right panel:1100 rpm. c) hexagonally ordered aggregates of spinning 570 μ m disks at 1100 rpm. d) Various dynamic patterns formed by rotating disks suspended at ethylene glycol- water interface. All disks are spinning around their centers at $\omega=700$ rpm. e)Reversible dynamic assembly depending on the rotational speed of the ω . Reproduced from [53].

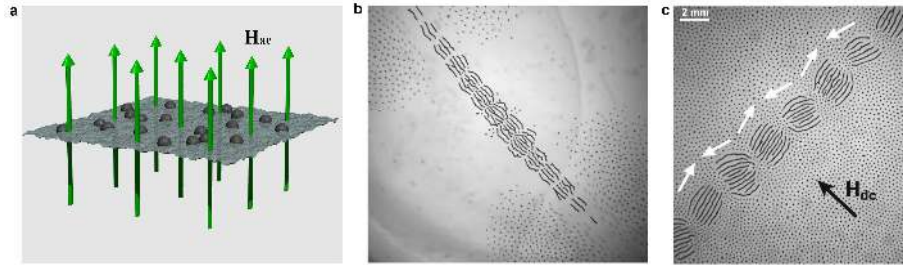


Figure 2: Dynamic self-assembly of torque-driven magnetic particles at liquid interface. a) Schematics of the external magnetic field forcing. Alternating magnetic field is applied perpendicular to the liquid interface. Torques acquired by particles are transferred to the interface resulting in strong vortical flows around each particle and interface oscillations. b) Dynamic multi-segmented self-assembled pattern (magnetic snake) promoted by an alternating magnetic field (110 Oe, 50 Hz.). c) Unusual magnetic ordering of the magnetic snake. White arrows designate directions of the magnetization vector at corresponding segments. Segments composed of ferromagnetically ordered chains of particles are antiferromagnetically ordered to each other. The structure was generated by a 110 Oe, 50 Hz magnetic field. Reproduced from Ref. [45, 55, 43]

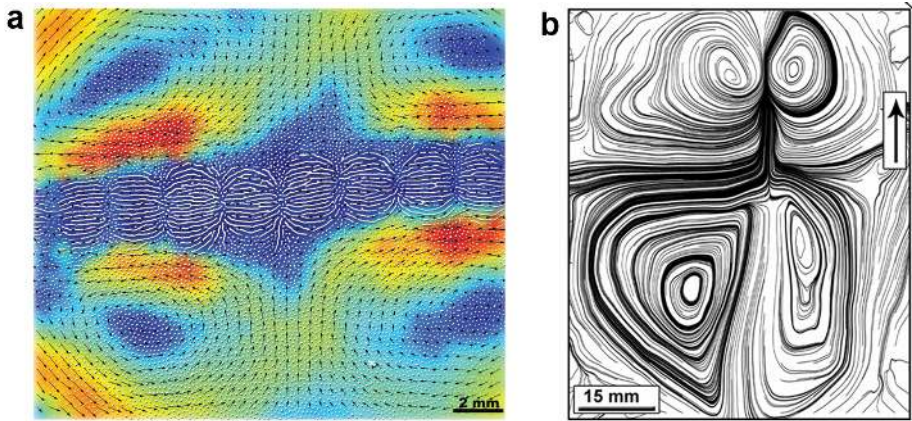


Figure 3: Induced interface hydrodynamic flows by active magnetic particles. a) Flow patterns generated by dynamically assembled magnetic snakes. b) stream lines of the flows produced by self-propelled magnetic snake. The arrow depicts the direction of swimming. Swimmers spontaneously brake the symmetry of the induced quadrupole vortex structure [39]. Reproduced from Ref. [58, 39].

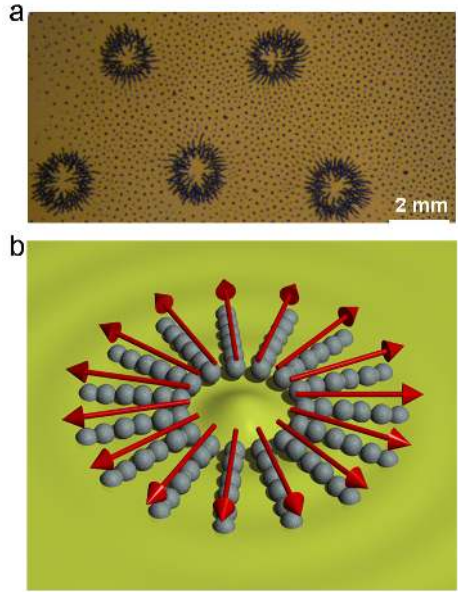


Figure 4: Dynamically assembled asters at liquid-liquid interface. a) array of asters. b) Magnetic order of an aster. Two flavors of magnetic order are permissible: magnetic moments pointing inward and outward (pictured). Reproduced from Ref. [37].

1
2
3
4
5
6
7
8
9
10
11
12
13
14
15
16
17
18
19
20
21
22
23
24
25
26
27
28
29
30
31
32
33
34
35
36
37
38
39
40
41
42
43
44
45
46
47
48
49
50
51
52
53
54
55
56
57
58
59
60
61
62
63
64
65

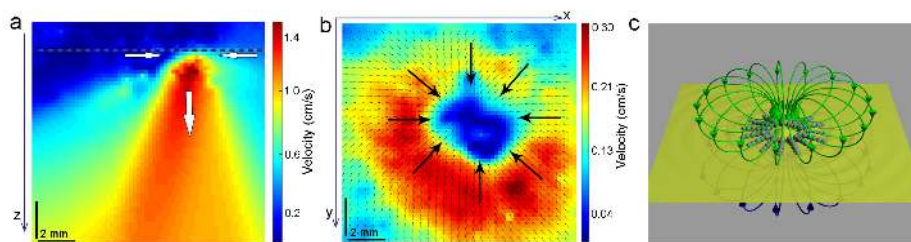


Figure 5: Induced hydrodynamic flows by self-assembled asters. a) Flow velocity field generated by an aster in the bottom liquid layer (vertical slice) obtained by particle image velocimetry. The dashed line depicts the position of the interface, frequency of the alternating magnetic field is 15Hz. Flow direction is shown schematically by arrows. b) Horizontal slice of the flow velocity generated by the aster. Arrows show flow direction. The slice was taken 0.5mm below the interface. c) schematics of hydrodynamic streaming flows induced by an aster structure. Toroidal flows accompany each aster with the liquid jets pointing perpendicular to the interface. Reproduced from Ref. [37].

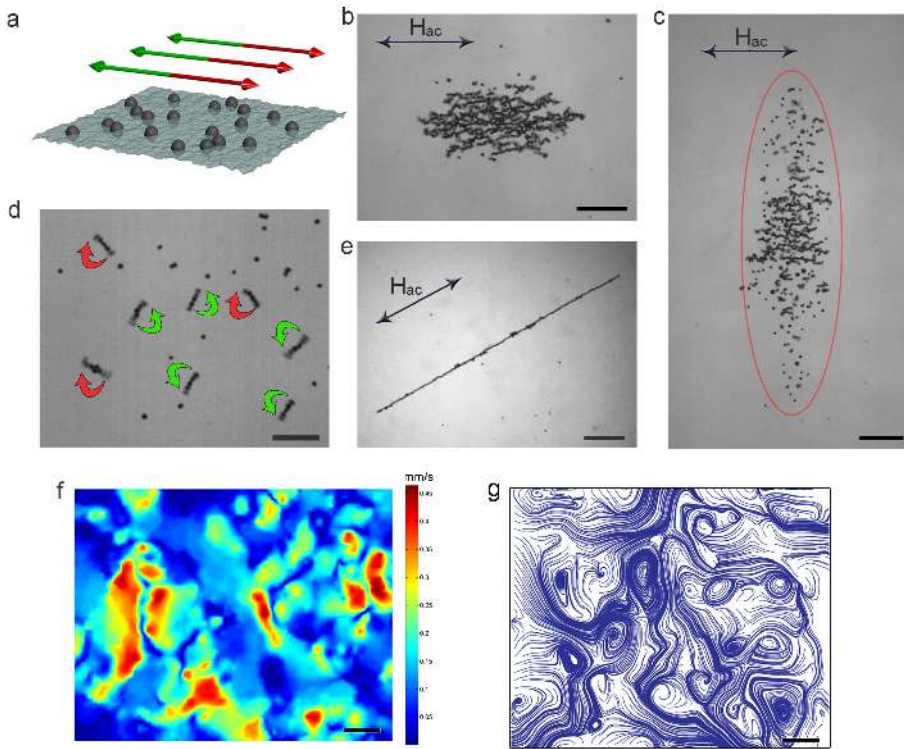


Figure 6: Active dynamics and self-assembly of ferromagnetic suspension at the air-liquid interface with planar magnetic field actuation. a) schematics of the experiment. Uniaxial magnetic field is applied parallel to the air-liquid interface. b) Loose pulsating cluster observed at 20 Hz, 27 Oe magnetic field. Scale bar is 2 mm. (e) Dynamic particle-thick wire formed at 180 Hz, 40 Oe magnetic field. Scale bar is 2 mm. (c) A snapshot of a perpendicular cloud consisting of continuously rearranging short chains. The cloud is extended perpendicular to the axis of the applied magnetic field (40 Hz, 40 Oe) in striking contrast to the cluster phase or dynamic wires. Scale bar is 2 mm. (d) Spinner phase formed at 50 Hz, 29 Oe magnetic field. Short chains of particles rotate in either direction with the frequency of the applied magnetic field. Clock- and anti-clock-wise spinners are illustrated by arrows. Scale bar is 1 mm. f) A typical snapshot of a magnitude of the hydrodynamic flow velocity field generated by spinners at the air-liquid interface. The in-plane applied alternating magnetic field is 29 Oe, 70 Hz. Scale bar is 2mm. (g) A typical streamline pattern of hydrodynamic surface flows. Spinners produce a complex time dependent vorticity distribution at the liquid interface. Scale bar is 2 mm. Reproduced from Ref. [37].

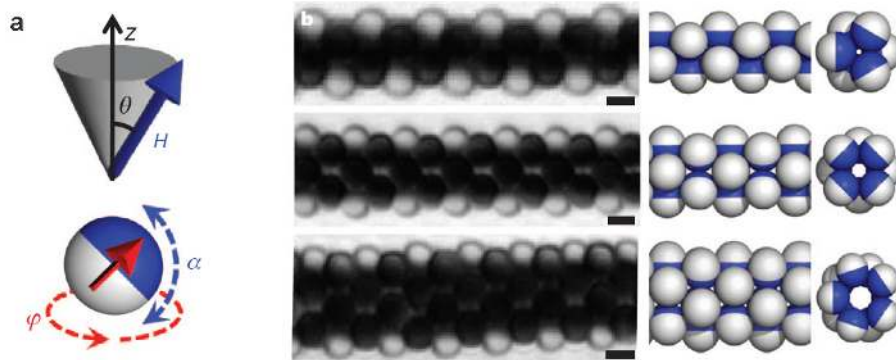


Figure 7: Active synchronisation-induced self-assembly in suspension of magnetic Janus particles. a) Janus particle with the director (red) rotating around precession axis in a precessing magnetic field. b) Experimental images and corresponding model of self-assembled microtubes. Reproduced from Ref. [41].

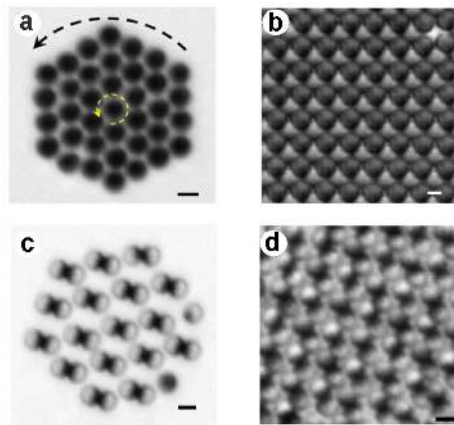


Figure 8: Assembly of magnetic Janus particles in rotating magnetic fields. a) 2d hexagonal crystal in rotating magnetic field (20Hz, 2mT). Black arrow indicates the rotation of the entire crystal. b) Planar crystal with a square symmetry formed by $3 \mu\text{m}$ Janus colloids in 20Hz, 5mT rotating field. Scale bar is $2 \mu\text{m}$. c) self-assembled crystal of dicolloids. d) snapshot of a square lattice dicolloid assembly. Scale bar is $2 \mu\text{m}$. Reproduced from Ref. [65].

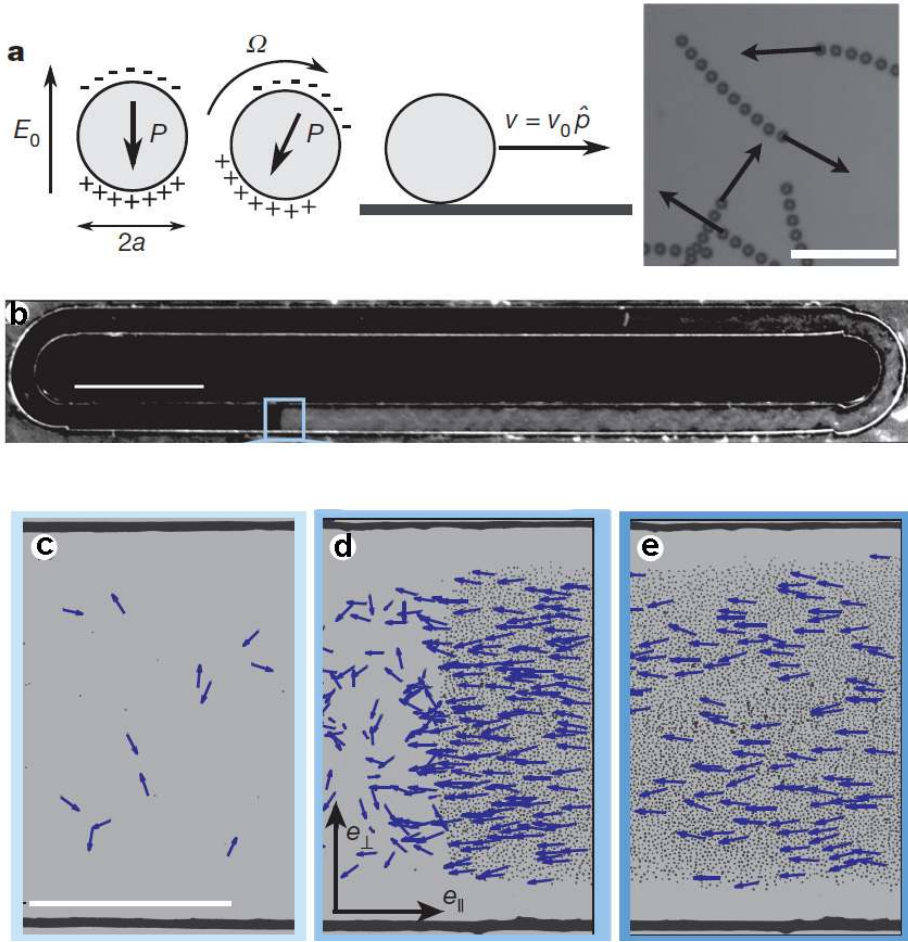


Figure 9: Colloidal rollers dynamics facilitated by Quincke rotations. a) Sketch of the mechanism of the Quincke rotation and resulting propulsion. b) Dark-field image of population of rollers formed a density band propagating along the predefined enclosed racetrack. c) close-up view of the density band. The arrows correspond to the rollers velocities. Reproduced from Ref. [72].

1
2
3
4
5
6
7
8
9
10
11
12
13
14
15
16
17
18
19
20
21
22
23
24
25
26
27
28
29
30
31
32
33
34
35
36
37
38
39
40
41
42
43
44
45
46
47
48
49
50
51
52
53
54
55
56
57
58
59
60
61
62
63
64
65

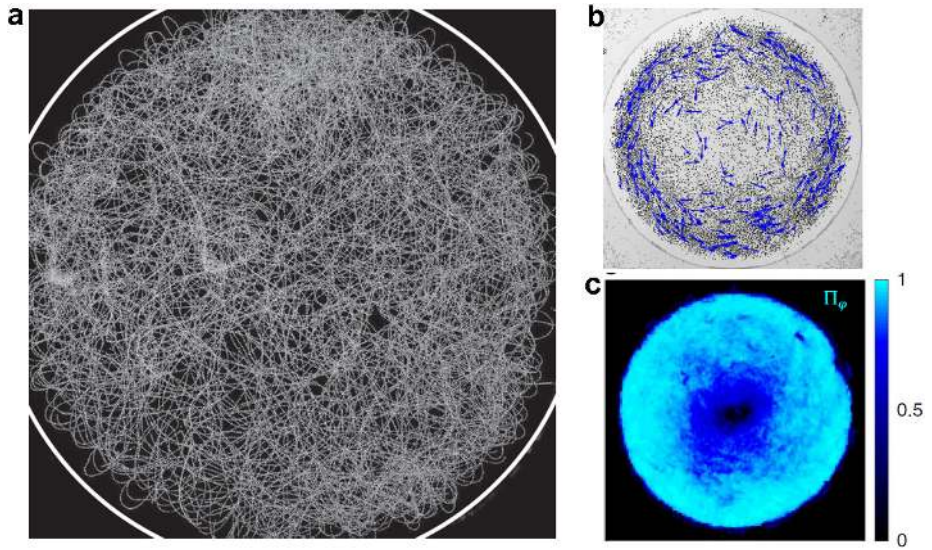


Figure 10: Colloidal rollers inside a circular cavity. a) superimposed images of a dilute ensemble of rollers. Colloids follow a persistent random walk. b) snapshot of a dynamic vortex state of rollers. Arrows represent the instantaneous speeds of rollers. c) time-averaged polarization field. Reproduced from Ref. [73].

1
2
3
4
5
6
7
8
9
10
11
12
13
14
15
16
17
18
19
20
21
22
23
24
25
26
27
28
29
30
31
32
33
34
35
36
37
38
39
40
41
42
43
44
45
46
47
48
49
50
51
52
53
54
55
56
57
58
59
60
61
62
63
64
65

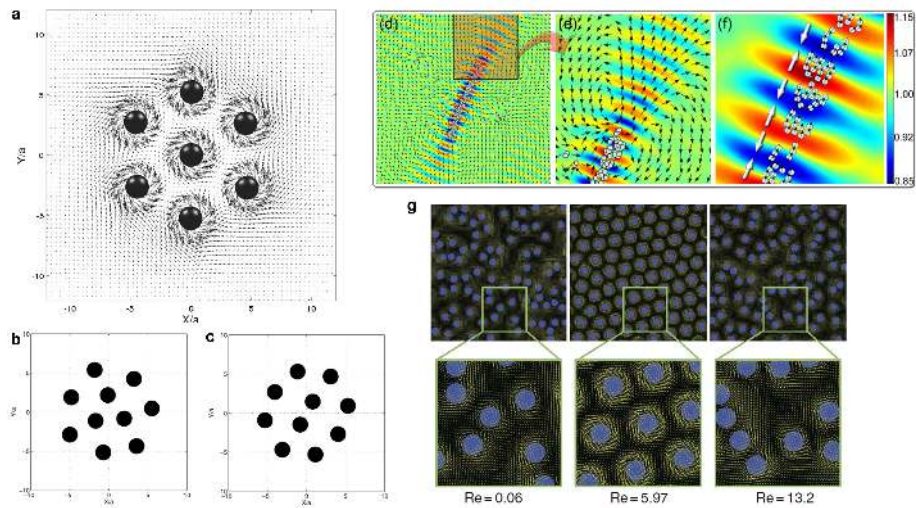


Figure 11: Simulation of active rotators. a) fluid velocity field of the stable aggregate of rotating spheres ($N=7$, $Re=2$). b,c) stable dynamic patterns for $N=10$ at $Re=2$. d) flow generated by magnetic snake in the entire domain. Background color reflects the amplitude of self-induced surface wave [2]. e) flow pattern in the vicinity of the snake's tail. f) antiferromagnetic order of the particles within the snake structure. Reproduced from Ref. [88, 89, 86].